

The Thermal Expansion of ScAlO_3 – A Silicate Perovskite Analogue

R.J. Hill¹ and Ian Jackson²

¹ CSIRO Division of Mineral Products, PO Box 124, Port Melbourne, Victoria 3207, Australia

² Research School of Earth Sciences, The Australian National University, GPO Box 4, Canberra, ACT 2601, Australia

Abstract. The crystal structure of ScAlO_3 has been refined at temperatures up to 1100° C on the basis of x-ray powder diffraction data. The thermal expansion is adequately described by a Grüneisen-Debye model with the elastic Debye temperature and an effective Grüneisen parameter of 1.6. The volumetric thermal expansion of 3.0% between 10 and 1100° C, corresponding to a mean thermal expansion coefficient of $2.7 \times 10^{-5} \text{ K}^{-1}$, is entirely attributable to the expansion of the AlO_6 octahedra. The interoctahedral angles, though not fixed by symmetry, do not vary significantly with temperature – indicating that the expansivities of the constituent AlO_6 and distorted ScO_8 polyhedra are well matched. Similar considerations of polyhedral expansivity suggest thermal expansion coefficients of $\sim 2 \times 10^{-5} \text{ K}^{-1}$ for cubic CaSiO_3 perovskite and a value between $2 \times 10^{-5} \text{ K}^{-1}$ and $4 \times 10^{-5} \text{ K}^{-1}$ for MgSiO_3 perovskite. The lower value is consistent with the reconnaissance measurements for $\text{Mg}_{0.9}\text{Fe}_{0.1}\text{SiO}_3$ (Knittle et al. 1986) below 350° C, with low-temperature measurements of single-crystal MgSiO_3 (Ross and Hazen 1989), and with the results of some recent calculations. The markedly greater expansivity ($\sim 4 \times 10^{-5} \text{ K}^{-1}$ measured at higher temperatures (350–570° C) by Knittle et al. is inconsistent with the simple Grüneisen-Debye quasiharmonic model and may reflect the marginal metastability of the orthorhombic perovskite phase. Under these circumstances, extrapolation of the measured expansivity is hazardous and may result in the underestimation of lower mantle densities and the drawing of inappropriate inferences concerning the need for chemical stratification of the Earth's mantle.

1. Introduction

Recent calculations for the densities for alternative compositional models for the Earth's lower mantle have focused attention on the thermal expansion of silicate perovskites. In particular, it has been demonstrated that the simplest model – that with uniform chemical composition throughout the mantle – is viable only if the mean thermal expansion coefficient for ferromagnesian silicate perovskite does not significantly exceed $3 \times 10^{-5} \text{ K}^{-1}$ (Jackson 1983; Jeanloz and Thompson 1983).

A pioneering study by Knittle et al. (1986) of $\text{Mg}_{0.9}\text{Fe}_{0.1}\text{SiO}_3$ perovskite yielded a thermal expansion coefficient α of $4 \times 10^{-5} \text{ K}^{-1}$ in conflict with this requirement.

It was therefore inferred that the mantle must be compositionally layered – the lower mantle being enriched relative to the upper mantle in silica or iron, or both. The very high pressures (> 23 GPa) required to stabilize this silicate perovskite pose twin problems for the measurement of its thermal expansion. Firstly, the perovskite material was available for the Knittle et al. study via diamond-cell synthesis only in minute quantities. Secondly, and more importantly, the measurements must be conducted under conditions of marginal metastability of the perovskite phase – temperatures of only $\sim 570^\circ \text{C}$ being sufficient to cause reversion to the low-pressure pyroxene structure. A recent x-ray diffraction study of single-crystal MgSiO_3 perovskite was restricted to temperatures below 130° C by pervasive twinning which precluded the accurate determination of unit cell dimensions at higher temperatures (Ross and Hazen 1989).

Owing to these inevitable limitations on the study of the silicate perovskite, it is potentially profitable to measure the thermal expansion of close structural analogues which are stable at lower pressures. In terms of molar volume and crystal structure, the *closest* such analogue is ScAlO_3 perovskite (Reid and Ringwood 1975) which can be synthesized in relatively large-volume piston-cylinder apparatus at ~ 3 GPa and 1000° C (Liebermann et al. 1977). Polycrystalline specimens grown under such conditions have provided for the measurement of elastic wave velocities (Liebermann et al. 1977). The availability of microcrystals has allowed refinement of the crystal structure (Sinclair et al. 1979) and measurement of the single-crystal elastic constants by Brillouin spectrometry (Bass 1984). The much closer proximity of its stability field is expected to allow the study of the thermal expansion of ScAlO_3 to much higher temperatures than is possible for its silicate perovskite analogue.

2. Experimental Details and Results

The development by Liebermann et al. (1977) of hot-pressing procedures for the fabrication of sintered polycrystals of high acoustic quality left a legacy of several poorly sintered specimens of ScAlO_3 perovskite. These samples, which were unsuitable for ultrasonic characterisation, each provided ~ 50 – 80 mg of material for the present high-temperature x-ray powder diffraction study. These samples were crystallized in platinum capsules from a homogeneous equimolar mixture of the oxides Al_2O_3 and Sc_2O_3 in amorphous

Table 1. Cell dimensions for ScAlO₃ perovskite

	Temp(°C)	a(Å)	b(Å)	c(Å)	V(Å ³)
Sinclair et al. (1979)	20	4.9355(3)	5.2313(3)	7.2007(5)	185.92(3)
Bass (1984)	*	4.9357(5)	5.2312(5)	7.2017(3)	185.95(4)
Reid and Ringwood (1975)	*	4.933(3)	5.226(3)	7.193(5)	185.4(4)
Present study:					
Continuous-scan powder data					
Pure sample # 1	10	4.934(3)	5.226(3)	7.192(3)	185.5(3)
Pure sample # 1	200	4.942(2)	5.232(6)	7.207(2)	186.4(3)
Pure sample # 1	400	4.953(2)	5.243(2)	7.227(2)	187.7(2)
Pure sample # 1	600	4.965(2)	5.251(2)	7.240(2)	188.8(2)
Pure sample # 1	800	4.974(2)	5.257(2)	7.252(2)	189.6(2)
Pure sample # 1	1000	4.984(2)	5.265(2)	7.269(2)	190.7(2)
Pure sample # 1	1200	4.995(3)	5.272(3)	7.288(3)	191.9(3)
Step-scan (Rietveld) powder data:					
Pure sample # 2	10	4.9354(1)	5.2302(2)	7.2012(2)	185.89(2)
Impure sample # 3	10	4.9370(2)	5.2321(2)	7.2045(2)	186.10(2)
Impure sample # 3	500	4.9597(2)	5.2471(2)	7.2353(2)	188.29(2)
Impure sample # 3	800	4.9767(2)	5.2584(2)	7.2604(2)	190.00(2)
Impure sample # 3	1100	4.9930(2)	5.2690(2)	7.2846(2)	191.64(2)

* room temperature

form (Reid and Ringwood 1975). Conditions for the crystallisation and hot-pressing of the various specimens ranged from 3 GPa and 1150° C in piston-cylinder apparatus to

6.5 GPa and 1000° C in girdle apparatus. Preliminary x-ray powder diffraction data indicated that each of these specimens was predominantly ScAlO₃ perovskite with minor impurities including platinum and possibly unreacted component oxides.

In the first exploratory part of the project, continuous-scan powder diffraction data ($6^\circ < 2\theta < 90^\circ$) for a relatively pure ScAlO₃ perovskite specimen were collected at 200° intervals between 10 and 1200° C using a Rigaku high-temperature diffractometer and CuK α radiation. Unit cell dimensions were obtained from the positions of the peak centroids (estimated manually) using a least-squares procedure; no internal standard was used. The resulting cell dimensions are presented in Table 1 and Fig. 1. The room temperature values are very close to those of Reid and Ringwood (1975) but are all slightly smaller than the single-crystal values of Sinclair et al. (1979) and Bass (1984). The cell dimensions vary approximately linearly with increasing temperature. Pronounced anisotropy is evident – with similar average linear expansivities of $\sim 1.0 \times 10^{-5} \text{ K}^{-1}$ parallel to *a* and *c*, but a substantially lower expansivity of $\sim 0.7 \times 10^{-5} \text{ K}^{-1}$ parallel to *b* (see discussion below).

Further information was subsequently obtained for a second specimen of lesser purity (see Fig. 2) in the form of step-scan powder diffraction data. These data were also collected on the Rigaku diffractometer in continuous-scan ($0.5^\circ \text{ min}^{-1}$) mode, but with the contents of the timer/scaler sampled every $0.04^\circ 2\theta$, tantamount to a step counting time of about 5 s. For this sample, data were collected between 32 and $91^\circ 2\theta$ at temperatures of 10, 500, 800 and 1100° C. Each of these digitised powder diffraction patterns was analysed with the full-profile Rietveld method (Rietveld 1969) using the program LHPM (Hill and Howard 1986). This procedure permits the refinement of unit cell dimensions and crystal structure parameters simultaneously by fitting a calculated profile to the entire observed diffraction pattern, step by step. Details of the refinement strategy are provided by Hill (1985). Contributions from residual reactant phases, the Pt sample holder and heating element at

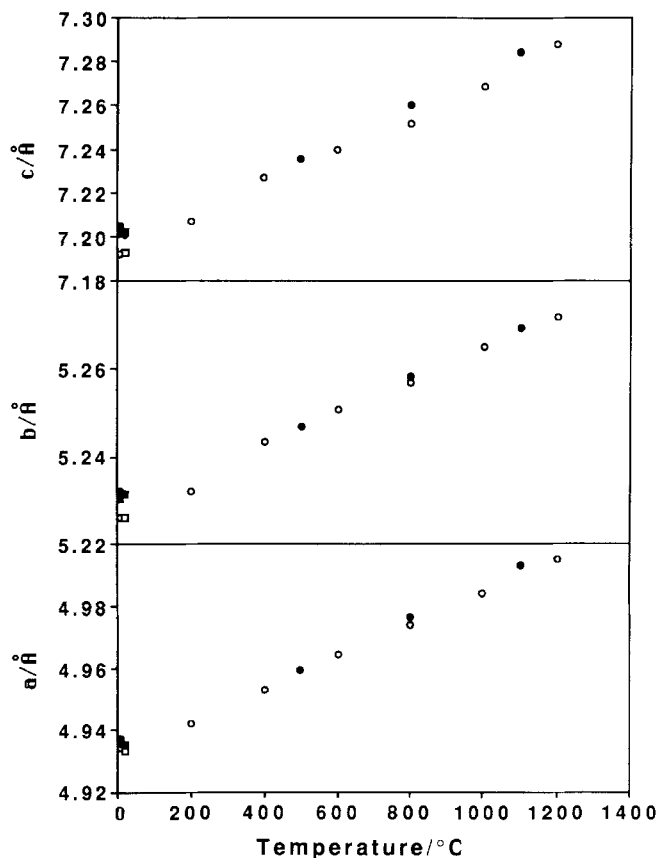


Fig. 1. Temperature dependence of the unit cell dimensions for ScAlO₃ perovskite. *Open circles*: continuous-scan powder measurements; *filled circles and filled triangles*: step-scan (Rietveld) powder refinement; *open squares*: Reid and Ringwood (1975); *filled squares*: Bass (1984); *open diamonds*: Sinclair et al. (1979)

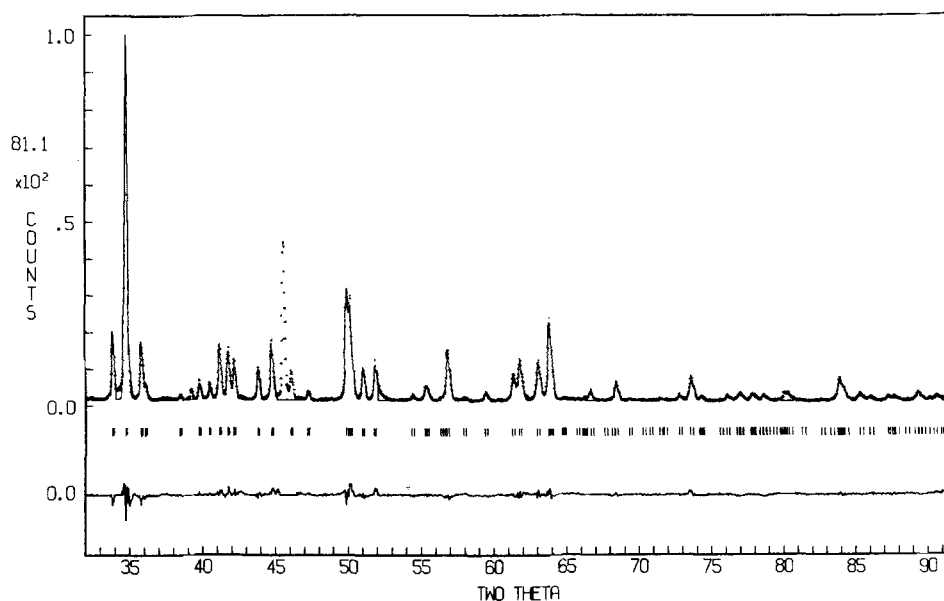


Fig. 2. Rietveld refinement powder diffraction profiles for ScAlO_3 perovskite at 1100°C . The observed step-scan data are indicated by *dots*, the calculated profile by the *continuous line* overlying them, and the 'difference' between the two, by the lower continuous curve. The positions of all Bragg peaks (including α_1 and α_2 components) are shown by the row of vertical tick marks below the observed/calculated profiles. Peaks due to the heating element and sample stage at 39 , 46 , 52 , 66 and $80^\circ 2\theta$ have been excluded from the calculated profile. Excluded regions have the calculated curve set equal to the background value

Table 2. ScAlO_3 perovskite structure refinements (space group: $Pbnm$ (62))

Parameter	Reid and Ringwood (1975)	Sinclair et al. (1979)	Present Study			
			10°	500°	800°	1100°
Sc <i>x</i>	0.974(4)	0.9793(1)	0.9775(3)	0.9786(3)	0.9797(3)	0.9813(3)
Sc <i>y</i>	0.072(4)	0.0701(1)	0.0700(2)	0.0690(2)	0.0680(2)	0.0676(2)
Sc $B(\text{\AA}^2)$	0.4	0.35	0.46(5)	0.75(4)	0.68(4)	0.96(4)
Al <i>B</i>	0.4	0.29	0.23(6)	0.25(5)	0.09(5)	0.49(5)
O1 <i>x</i>	0.133(11)	0.1196(3)	0.1252(8)	0.1283(9)	0.1241(6)	0.1250(6)
O1 <i>y</i>	0.446(12)	0.4551(3)	0.4462(8)	0.4443(7)	0.4464(7)	0.4478(7)
O1 $B(\text{\AA}^2)$	0.4	0.34	-0.02(10)	0.60(10)	0.36(8)	0.08(8)
O2 <i>x</i>	0.691(8)	0.6906(2)	0.6935(6)	0.6909(5)	0.6925(4)	0.6919(5)
O2 <i>y</i>	0.312(9)	0.3061(2)	0.3055(5)	0.3048(5)	0.3064(4)	0.3063(5)
O2 <i>z</i>	0.075(6)	0.0611(1)	0.0625(3)	0.0631(3)	0.0623(3)	0.0621(3)
O2 $B(\text{\AA}^2)$	0.4	0.37	-0.61(7)	-0.19(7)	-0.40(6)	-0.10(7)
Octahedron						
Al-O1(\AA)	2×1.935	2×1.9090	2×1.9249	2×1.9396	2×1.9379	2×1.9447
Al-O2(\AA)	2×1.892	2×1.8853	2×1.8783	2×1.8994	2×1.8928	2×1.9007
volume*(\AA^3)	9.562	9.158	9.236	9.400	9.430	9.514
Linkages						
Al-O1-Al($^\circ$)	137	141.1	138.7	137.7	139.0	138.9
Al-O2-Al($^\circ$)	138	142.8	142.9	142.4	142.7	142.6
Unit <i>a</i> (\AA)	4.933(3)	4.9355(3)	4.9370(2)	4.9597(2)	4.9767(2)	4.9930(2)
Cell <i>b</i> (\AA)	5.226(3)	5.2313(3)	5.2321(2)	5.2471(2)	5.2584(2)	5.2690(2)
Cell <i>c</i> (\AA)	7.193(5)	7.2007(5)	7.2045(2)	7.2353(2)	7.2604(2)	7.2846(2)
<i>R</i> (%)	11.6	2.8	3.6	3.2	3.7	3.9

* Approximated by four-thirds of the product of the three distinct Al-O distances

about 39 , 46 , 52 , 66 and $80^\circ 2\theta$ were excluded from the analysis. Scattering factors for ionized atoms were taken from International Tables for X-ray Crystallography (1974). Starting values for refinement of the structure in space group $Pbnm$ were taken from Sinclair et al. (1979).

Almost all of the positional parameters of the structure refined at 10° (Table 2) are in close agreement with those obtained in the single-crystal study of Sinclair et al. (1979).

The only exceptions are the *x*- and *y*-coordinates of O1 – which were also poorly determined in the room-temperature integrated-intensity powder study of Reid and Ringwood (1975). This atom may be problematical because (i) its position is sensitive to the overall stoichiometry of the compound, (ii) it has phase relationships which cause it to have relatively little effect on the observed diffraction maxima, or (iii) preferred orientation problems contribute

to the parameters of this atom more than the others (although the profile refinements undertaken in the present study incorporate a correction for this potential source of error).

The individual isotropic thermal vibration parameters (B) are somewhat unstable, especially for both O atoms, but they are not totally unreasonable considering the limited range of diffraction data collected, the contamination of the pattern by peaks from the heating element, the sample impurity level, and the fact that the single crystal values are themselves quite small. The agreement indices, R , are also small, significantly better than that obtained by Reid and Ringwood, but not quite as good as the Sinclair et al. value of 2.8%. All of this suggests that the results are reliable. Strikingly similar refined structures have been described by Yamanaka et al. (1987) in a recent study of single-crystal ScAlO_3 perovskite to 650° C.

The temperature dependence of the cell dimensions obtained from the present structure refinements is compared with the integrated intensity results in Table 1 and Fig. 1. Overall, the two studies are in good agreement. The slightly different absolute values of the cell dimensions probably reflect slight differences in the composition of the specimens. In this connection, it is interesting to note that a further pure specimen (# 2), which was inadvertently decomposed at high temperature, yielded cell dimensions at 10° C (Table 1) that are essentially identical to the single-crystal values of Sinclair et al. (1979). The relatively lower expansivity parallel to \mathbf{b} results in a modest reduction of the b/a ratio, from 1.060 at 10° C to 1.055 at 1100° C, as in the other orthorhombic perovskites (Liu et al. 1988; Liu and Liebermann 1988). The other measure $c/a\sqrt{2}$ of the distortion of the pseudocubic subcell is essentially temperature independent at a value of 1.032. Moreover, the high-temperature structure refinements of Table 2 indicate that the expansion is essentially homogeneous within the unit cell. Of particular interest is the fact that the angles through which the chains of corner-connected octahedra are kinked are independent of temperature. The 3.0% expansion of the unit cell between 10 and 1100° C is *quantitatively* explained by expansion of the constituent AlO_6 octahedra.

3. Analysis of the Volumetric Thermal Expansion

The volumetric expansion data deriving from both the integrated intensity and full profile measurements are plotted in Fig. 3. The fractional increase in cell volume $V(T)$ from the reference temperature T_R (10° C) to temperature T varies approximately linearly with temperature. The best fitting slopes, along with 2σ uncertainties, for the integrated intensity and full profile data are $(2.89 \pm 0.18) \times 10^{-5} \text{ K}^{-1}$ and $(2.60 \pm 0.17) \times 10^{-5} \text{ K}^{-1}$, respectively.

Grüneisen's theory has been widely and successfully employed in the analysis of thermal expansivity, as follows. For thermal expansion at zero pressure, the thermal pressure

$$P = \gamma E/V \quad (1)$$

required to maintain constant volume V while heating from 0 K to temperature T , and the (negative) pressure required to expand the static lattice (at 0 K) from V_0 to V , sum to zero. Derivation of an expression for the latter pressure, involving K_0 and dK_0/dP , by retention only of the first-

and second-order terms in the Taylor expansion of VdU/dV in powers of $V-V_0$, yields

$$V(T)/V_0 = [2k + 1 - (1 - 4kE(T)/Q)^{1/2}]/2k \quad (2)$$

where $U(V)$ is the energy of the static lattice, $k = (dK_0/dP - 1)/2$, $Q = K_0 V_0/\gamma$ and K_0 and dK_0/dP are, respectively, the isothermal bulk modulus at 0K and its first pressure derivative (Suzuki et al. 1979). The thermal energy E is customarily approximated by the Debye formula viz

$$E(\theta_D, T) = 45 RT(T/\theta_D)^3 \int_0^{\theta_D/T} x^3 dx / (e^x - 1) \quad (3)$$

for five atoms per formula unit of ScAlO_3 . Since equation (2) holds at all temperatures, including the reference temperature T_R , we may write:

$$V(T)/V(T_R) = [2k + 1 - (1 - 4kE(\theta_D, T)/Q)^{1/2}] / [2k + 1 - (1 - 4kE(\theta_D, T_R)/Q)^{1/2}] \quad (4)$$

The parameters required in the calculation or modeling of the thermal expansion of ScAlO_3 perovskite have been assembled in Table 3. The Grüneisen parameter γ is treated as an adjustable parameter expected to be of order 2. No attempt has been made to correct measured or inferred values of V_0 , K_0 and dK_0/dP to 0 K. Of these parameters, V_0 and K_0 appear only in combination with γ in $Q = K_0 V_0/\gamma$, the modest error incurred in the choice of K_0 and V_0 is therefore accommodated by variation of the adjustable parameter γ . The volumetric expansion calculated from equation (4) is very insensitive to variation of the assumed value of dK_0/dP (as shown below) so that the choice of its value is not critical.

A trial calculation with the parameters of Table 3 and γ set equal to the Dugdale-MacDonald value ($\gamma_{DM} = (dK_0/dP - 1)/2 = 2$) yielded a slightly concave upward curve for $V(T)/V(T_R) - 1$ versus temperature with systematically higher expansion than observed (e.g. 0.043 versus 0.035 observed at 1200° C).

The sensitivity of the calculated expansion to variation of the model parameters was then explored as a guide in the improvement of the model. Since $4kE/Q < 0.4$ for $T < 1500$ K, a good approximation to the calculated expansion is obtained by retaining the first two terms only in a series expansion of $(1 - 4kE/Q)^{1/2}$. Thus,

$$V(T)/V(T_R) - 1 \approx [E(T) - E(T_R)]/Q = \gamma [E(T) - E(T_R)]/K_0 V_0 \quad (5)$$

Table 3. Parameters for the Grüneisen-Debye analysis of thermal expansion for ScAlO_3 perovskite

Parameter	Value	Source
V_0	$2.80 \times 10^{-5} \text{ m}^3/\text{mol}$	Sinclair et al. (1979)
K_0	249 GPa	Bass (1984)
θ_D	900 K	Bass (1984) ^a
dK_0/dP	5	Jones (1979) ^b
γ	adjustable	

^a θ_D calculated from the compressional and shear wave velocities for an isotropic polycrystalline aggregate using a well known relationship (e.g. Anderson et al. 1968)

^b By analogy with other perovskites

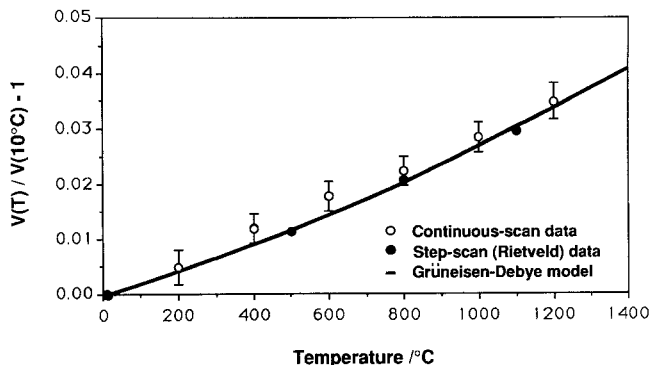


Fig. 3. Measured volumetric thermal expansion of ScAlO_3 perovskite (symbols as for Fig. 1) compared with an appropriate Grüneisen-Debye model with the parameters given in Table 3 and $\gamma = 1.6$

With K_0 and V_0 well constrained at room temperature and k absent from equation (5), it is clear that the expansion calculated from equation (4) is controlled by the assumed value of γ and, to a much lesser extent, θ_D . γ was therefore decreased to 1.6 (with θ_D held constant at the ‘elastic’ value of 900 K) to produce a reasonable overall fit to the data (Fig. 3). The trade-off between θ_D and γ is such that $\theta_D = 800$ K and $\gamma = 1.57$ yields an essentially indistinguishable fit to the data.

It is concluded that the measured thermal expansion of ScAlO_3 perovskite is readily reconciled with a Grüneisen-Debye model via a plausible value of 1.6 ± 0.1 for the Grüneisen parameter.

4. Discussion

The thermal expansion of a three-dimensional framework of corner-connected BO_n polyhedra can be viewed as the sum of contributions arising from the expansion of the framework-forming polyhedron and from temperature dependence of the $B\text{-O-B}$ angles through which the polyhedra are linked (e.g. Hazen and Finger 1982). The relative magnitudes of these two contributions were examined by Megaw (1971) in a comparison of the thermal expansion for selected pairs of structures based upon the same coordination polyhedron, with and without control (via symmetry) of the orientation of the polyhedra. It was concluded that

“framework structures in which polyhedra are tilted away from symmetrical orientations always show larger mean linear expansions than similar structures in which the orientations are fixed by symmetry”.

ScAlO_3 perovskite clearly violates this rule. The Al-O1-Al (Sinclair et al. 1979, Fig. 1) and Al-O2-Al angles (Fig. 4) are *not* fixed by symmetry, and yet, do not vary significantly between 10 and 1100°C (Table 2). The 3.0% volumetric expansion between 10 and 1100°C is therefore entirely attributable to the expansion of the AlO_6 octahedra. A comparable expansion of 2.8% over the same temperature interval is observed (Skinner 1966) for corundum in which the orientations of the AlO_6 octahedra are fixed by face-sharing along c and by a symmetrical arrangement of shared edges within the octahedral layers normal to c .

The expansion of Sc_2O_3 with the cubic bixbyite structure (space group $Ia\bar{3}$) is 2.9% for the interval 20–1100°C (Skinner 1966) – similar to that for corundum. The MO_8 coordination cube of the parent fluorite structure (Wyckoff 1963)

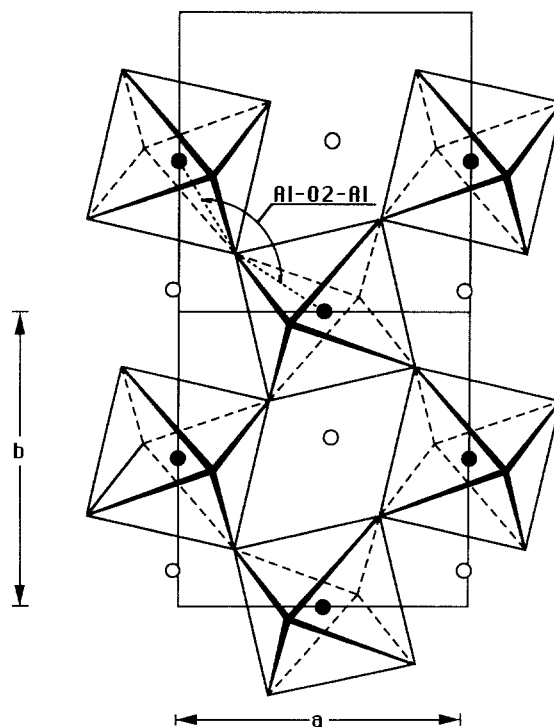


Fig. 4. The (001) layer of corner-connected AlO_6 octahedra in the structure of ScAlO_3 perovskite. The Al-O2-Al angle is indicated. Structure along [001] including the Al-O1-Al angle is illustrated in Fig. 1 of Sinclair et al. (1979). The filled and open circles represent, respectively, Al atoms at $z=0$ and Sc atoms at $z=0.25$. The oxygen atoms located at the shared corners of the AlO_6 octahedra are at $z=0.25, -0.06, +0.06$ and $+0.25$

is transformed into two different irregular ScO_6 coordination polyhedra in Sc_2O_3 by removal of two oxygen atoms from either end of one of either the body- or face-diagonals of the cube. The interatomic distances are 6×2.120 Å and 2×2.080 Å, 2×2.125 Å and 2×2.164 Å for Sc(1)-O and Sc(2)-O, respectively (Norrestam 1969). The orientations of these polyhedra are constrained by the sharing of all six of the edges, subparallel to the cubic axes, remaining from the MO_8 cube of the parent structure.

The similar, relatively small expansion coefficients for Sc_2O_3 and Al_2O_3 are consistent with well-established empirical correlations between thermal expansivity and Pauling bond strength, defined as z_c/n where z_c is the cation valence and n its coordination number. For structures in which polyhedral orientations are fixed, the proportionality:

$$\alpha \propto (z_c/n)^{-2} \quad (6)$$

provides a reasonable description of the observed expansion coefficients (Megaw 1971). The mean volumetric thermal expansion coefficient from room temperature to 1000°C for oxide polyhedra in a wide variety of structures is well approximated by the expression

$$\bar{\alpha}_{1000} = 9.87(0.75 - z_c/n) \times 10^{-5} \text{ K}^{-1} \quad (7)$$

due to Hazen and Prewitt (1977). A more widely applicable correlation favoured by Hazen and Finger (1982) yields, for oxide polyhedra:

$$\bar{\alpha}_{1000} = 1.21(z_c/n)^{-1} \times 10^{-5} \text{ K}^{-1} \quad (8)$$

The observation that the Al-O-Al angles in ScAlO_3 perovskite do not increase towards 180° with increasing tempera-

ture indicates that the expansivities of the constituent AlO_6 and ScO_8 polyhedra must be well matched. Such a match has already been noted between the expansivities of the AlO_6 and ScO_6 polyhedra in the respective oxides – consistent with the expansivity-bond strength systematics Eqs. (6–8). However, Eqs. (7) and (8) suggest that for ScO_8 polyhedra, expansivity substantially larger (by 50 and 33%, respectively) than for ScO_6 polyhedra should be expected. Two possible explanations are offered for the conflict between the observations for ScAlO_3 perovskite and the predictions of the empirical systematics:

(i) Although Eqs. (7) and (8) represent satisfactory descriptions of the thermal expansivity of a wide variety of polyhedra, they appear to overestimate the sensitivity of the expansivity to change of coordination number for a given $M\text{-O}$ pair. For example scrutiny of Table 6.3 of Hazen and Finger (1982) indicates a range $(2.7\text{--}4.8) \times 10^{-5} \text{ K}^{-1}$ with a mean of $4.2 \times 10^{-5} \text{ K}^{-1}$ for the volume expansivity for 20 different MgO_6 polyhedra. The only datum for an MgO_8 polyhedron (from pyrope garnet), $3.9 \times 10^{-5} \text{ K}^{-1}$, lies within the range of expansivities observed for MgO_6 polyhedra and is not significantly different from the mean. Similarly, for CaO_6 and CaO_8 polyhedra, expansivity ranges of $(3.9\text{--}5.7) \times 10^{-5} \text{ K}^{-1}$ and $(3.0\text{--}4.8) \times 10^{-5} \text{ K}^{-1}$ are observed, with means of four observations in each case of $4.5 \times 10^{-5} \text{ K}^{-1}$ and $4.2 \times 10^{-5} \text{ K}^{-1}$, respectively.

(ii) A further issue in the case of ScAlO_3 is the ambiguity in the definition of the ScO_n coordination polyhedron. Distances between Sc and the 12 oxygen nearest neighbours range from 2.068 Å to 3.398 Å (Table 4). Sinclair et al. (1979) argued, on the basis of the break between 2.555 Å and 3.107 Å, for 8-coordination. Bond strength sums for 6, 8 and 12 neighbours are respectively 2.56, 2.85 and 2.95 – indicating the dominant role in bonding of the six nearest neighbours. The expansivity of the highly irregular ScO_8 polyhedron may thus be determined by the six shortest and strongest Sc-O bonds, in which case an expansivity comparable with those of the ScO_6 polyhedra in Sc_2O_3 would be expected.

Whatever the explanation, there can be no doubt that the expansivities of the AlO_6 and ScO_8 polyhedra of ScAlO_3 perovskite are well matched. The niobate perovskites in which the orientation of the Nb^{+5}O_6 octahedron is not fixed by symmetry (e.g. P-NaNbO_3 , Megaw 1971) represent the other extreme. Here, there is evidently a very large mismatch between the very low expansivity of the framework-forming Nb^{+5}O_6 octahedron with bond strength 5/6,

and the much larger expansivity expected of the distorted $A^{+1}\text{O}_8$ polyhedron with bond strength 1/8. The result is a significant contribution to the expansion of the structure from an increase in the Nb–O–Nb angle – driven by the mismatch in thermal expansivity between the framework-forming and ‘cage’ polyhedra.

5. Implications for Silicate Perovskites

The response of the structures of silicate perovskites to increasing temperature is difficult to study of the reasons outlined in the Introduction. Thus, the study of $\text{Mg}_{0.9}\text{Fe}_{0.1}\text{SiO}_3$ by Knittle et al. (1986) yielded only relatively imprecise determinations ($\pm 0.3\%$) of the unit cell volume and no information concerning structural variation within the unit cell. Grüneisen-Debye modeling of the data, in which all four parameters γ , θ_D , dK_0/dP and V_0 were allowed to vary, yielded a ‘best fit’ ($\gamma=1.77$, $\theta_D=525 \text{ K}$, $dK_0/dP=7$, $V_0=2.446 \times 10^{-5} \text{ m}^3 \text{ mol}^{-1}$) tabulated by Knittle et al. and plotted in their Fig. 1. (Note, however, that their equation for the volume at temperature T is in error (c.f. Eq. (2)) and that the expression for k should read $(dK_0/dP-1)/2$). Our calculations indicate that the Grüneisen-Debye model (2) with the Knittle et al. ‘best fit’ parameters systematically overestimates the measured thermal expansion except at the very highest temperatures (570° C) reached in their study.

We have therefore applied the modeling strategy, employed above for ScAlO_3 , to the Knittle et al. data, taking advantage of the availability of well-constrained values of K_0 ($246 \pm 5 \text{ GPa}$) and θ_D (1094 K) deriving from recently published elasticity data for single-crystal MgSiO_3 perovskite (Yeganeh-haeri et al. 1989). It proved impossible to obtain a satisfactory fit to the data across the full temperature range ($20\text{--}570^\circ \text{ C}$) with a constant value of γ (see also Anderson, 1988). Rather, the data, which define a trend of much greater curvature (concave upwards c.f. Fig. 3) in temperature-volumetric expansion space than is characteristic of the models, straddle a region bounded by the $\gamma=1.2$ and $\gamma=2.0$ models (θ_D , V_0 , K_0 and $dK_0/dP=5$ being fixed at their preferred values). Below 350° C , the data are well fitted by the $\gamma=1.2$ model; at 570° C , however, this model underestimates the measured expansion of 1.8% by approximately 40%.

Recognition of these difficulties presumably motivated the recent reanalysis (Jeanloz and Knittle 1989) of the expansivity data in terms of a more elaborate model. Allowance for the volume dependence of γ and θ_D increases the thermal pressure (and hence also the thermal expansion) calculated at high temperatures for the quasiharmonic model. Additional flexibility in the modeling of thermal expansion is provided by the incorporation (following Wallace) of a further anharmonic term proportional to $T^2 - T_0^2$ (with $T_0=300 \text{ K}$) which may contribute either positively or negatively to the thermal pressure. These two alternatives were encountered in modeling the thermal expansion of (Mg, Fe) SiO_3 perovskite and MgO , respectively (Jeanloz and Knittle 1989).

Our $\gamma=1.2$ model, which fits the $\text{Mg}_{0.9}\text{Fe}_{0.1}\text{SiO}_3$ data below 350° C and is consistent with the Ross and Hazen (1989) data for MgSiO_3 below 25° C , yields mean (extrapolated) expansivities of $2.0 \times 10^{-5} \text{ K}^{-1}$ and $2.4 \times 10^{-5} \text{ K}^{-1}$ for the intervals $20\text{--}730^\circ \text{ C}$ and $20\text{--}1300^\circ \text{ C}$, respectively. These values are much lower than those – $3.3 \times 10^{-5} \text{ K}^{-1}$ and $4 \times 10^{-5} \text{ K}^{-1}$, respectively – calculated directly from the measured expansion for the intervals $20\text{--}570^\circ \text{ C}$ and

Table 4. Sc-O distances in ScAlO_3 perovskite and associated bond strengths

Distance(Å) ^a	Bond Strength ^b
2.068	0.553
2 × 2.112	0.491
2.129	0.469
2 × 2.325	0.276
2 × 2.555	0.148
3.107	0.043
3.291	0.020
2 × 3.398	0.015

^a Sinclair et al. (1979)

^b Calculated from the bond length-bond strength relationship of Brown and Altermatt (1985)

180–570° C. It is thus clear that the pronounced increase in measured expansivity of (Mg, Fe) SiO₃ perovskite between 350 and 570° C cannot be accommodated by the simple Grüneisen-Debye model which adequately describes the thermal expansivity of a wide variety of oxides and silicates over much wider ranges of temperature. The more elaborate and flexible model used by Jeanloz and Knittle (1989), evidently provides a *superior fit* to the data. However, *extrapolation to much higher temperatures* of the term proportional to $(T^2 - T_0^2)$ which represents the additional thermal pressure (beyond quasiharmonic) is *fraught with danger*. In particular, it must be remembered that (Mg, Fe) SiO₃ perovskite is only marginally metastable at the higher temperatures attained during the thermal expansion measurements – reverting above 570° C to the low-pressure pyroxene structure. Perhaps large-amplitude vibrations associated with the imminent instability yield an anomalously large expansivity above 350° C; anomalously large expansivity is observed, for example, in α -quartz heated towards the $\alpha \rightarrow \beta$ transition (Skinner 1966). Interestingly, however, there is no evidence for this phenomenon in the expansion data for ScAlO₃ perovskite which decomposes to form a mixture of the constituent oxides after prolonged heating above 1200° C.

Even greater difficulties apply to the study of CaSiO₃ perovskite – an unquenchable cubic phase (Liu and Ringwood 1975). Any insight into the thermal expansion and structural variations of silicate perovskites gleaned from measurements on structural analogues or from theory is therefore of considerable value. Cell volumes determined within $\pm 0.01\%$ from the structure refinements on ScAlO₃ perovskite yield a mean thermal expansion coefficient of $2.7 \times 10^{-5} \text{ K}^{-1}$ for the temperature interval 10–1100° C. This expansion is entirely attributable to the expansion of the framework-forming AlO₆ octahedra – there being no significant variation with temperature of the interoctahedral Al-O-Al angles. The thermal expansion coefficient measured for ScAlO₃ perovskite is not directly transferable to silicate perovskites. However, the insight gained into the relative importance of octahedral expansion and variation of the interoctahedral angles may be applied to silicate perovskites as follows.

The measured volumetric thermal expansion for stishovite ($\bar{\alpha} = 2.0 \times 10^{-5} \text{ K}^{-1}$ for the interval 20–600° C – Ito et al. 1974), in which the interoctahedral angles associated with the sharing of edges normal to *c* and corner-sharing along [110] are fixed by symmetry, represents a lower bound for the expansivity of silicate perovskites. For the apparently cubic CaSiO₃ perovskite in which Si-O-Si angles are 180°, an expansivity of $\sim 2 \times 10^{-5} \text{ K}^{-1}$ is anticipated. Thermal expansion coefficients calculated by Wolf and Bukowinski (1987) and Hemley et al. (1987) range between 1.5 and $2.1 \times 10^{-5} \text{ K}^{-1}$ (Table 5) in reasonable accord with this prediction. If, however, CaSiO₃ perovskite were to prove to be only pseudocubic (with a nearly cubic unit cell but possibly highly distorted structure like CaGeO₃ – Sasaki et al. 1983), a significantly higher expansion coefficient would be expected.

For orthorhombic MgSiO₃ perovskite (space group *Pbnm*: Horiuchi et al. 1987) the thermal expansion coefficient may well exceed that of the SiO₆ octahedron – as suggested by the measurements of Knittle et al. (1986) at temperatures above 350° C. Being an $A^{2+}B^{4+}O_3$ compound, MgSiO₃ perovskite might be expected to behave in a manner intermediate between the $A^{3+}B^{3+}O_3$ and

Table 5. Volumetric thermal expansion coefficients for silicate perovskites – measured, calculated and predicted from structure-based systematics

	Expansion coefficient ^a	Temperature (interval)	References
MgSiO ₃			
Measured	4.0	180–570	Knittle et al. (1986)
	3.3	20–570	Knittle et al. (1986)
	2.0	20–730	$\gamma = 1.2$ fit to data < 350° C
	1.5	–196– 25	Ross and Hazen (1989)
Calculated	2.7	20–530	Wolf and Bukowinski (1987)
	1.9	25–730	Hemley et al. (1987)
	3.1	730	Hemley et al. (1989)
	4.4	25–730	Hemley et al. (1989)
	2.4	530	Navrotsky (1989)
	2.0–3.9	20–700	Range of polyhedral expansivities
CaSiO ₃			
Calculated	2.1	20–730	Wolf and Bukowinski (1987)
	1.5	25–730	Hemley et al. (1987)
	2.0	20–600	Polyhedral expansivity

^a Volumetric expansion coefficients (unit: 10^{-5} K^{-1}) are either ‘instantaneous’ values for specific temperatures (unit: °C) or mean coefficients for the indicated temperature interval

$A^{1+}B^{5+}O_3$ perovskites. Mg-O-Mg angles would be expected to increase with increasing temperature if the expansion of the distorted MgO₈ polyhedron were to exceed that of the SiO₆ octahedron. The only data for the expansivity of MgO₈ polyhedra derive from high-temperature refinements of the structure of pyrope garnet (Meagher 1975) which yield a mean volumetric expansion coefficient of $3.9 \times 10^{-5} \text{ K}^{-1}$ for the interval 25–750° C. It therefore seems probable that the Mg-O-Mg angles in MgSiO₃ perovskite will increase with increasing temperature, thereby contributing to the thermal expansion, and leading ultimately to the possibility of temperature-induced transitions to phases of higher symmetry (e.g. Wolf and Bukowinski 1987). The overall expansion coefficient for the orthorhombic phase should therefore lie between 2.0 and $3.9 \times 10^{-5} \text{ K}^{-1}$.

This prediction is compared in Table 5 with expansion coefficients deriving from the measurements of Knittle et al. (1986) and Ross and Hazen (1989) and the calculations of Wolf and Bukowinski (1987), Hemley et al. (1987, 1989) and Navrotsky (1989). The expansivities inferred from the measurements of Knittle et al. and Ross and Hazen cover the entire range allowed by considerations of polyhedral expansivity. Thus the expansivity of $2.0 \times 10^{-5} \text{ K}^{-1}$ associated with the $\gamma = 1.2$ model, which fits the data below 350° C, is comparable with the expansivity of the SiO₆ octahedron. The much higher value of $4 \times 10^{-5} \text{ K}^{-1}$ derived by Knittle et al. directly from their high temperature data (180–570° C) is similar to the expansivity of the MgO₈ polyhedron in pyrope. Most of the theoretical studies yield expansion coefficients which fall within the lower half $(1.9\text{--}3.1) \times 10^{-5} \text{ K}^{-1}$ of the range allowed by the measurements and the structural considerations discussed above. The expansion coefficient of $1.3 \times 10^{-5} \text{ K}^{-1}$ calculated by Cohen (1987) is lower even than the experimental value for stishovite (the putative value for the SiO₆ octahedron) and has recently been recognised

as a manifestation of inadequacies in the Potential-Induced Breathing model of the lattice dynamics of this complex structure (Hemley et al. 1989). Two alternative strategies, designed by these latter authors to suppress the influence of (artificially) unstable LO modes on the thermodynamic properties, yield expansivities of $2.3 \times 10^{-5} \text{ K}^{-1}$ (25° C) – $3.1 \times 10^{-5} \text{ K}^{-1}$ (730° C) and $4.4 \times 10^{-5} \text{ K}^{-1}$ (for 25 – 730° C), respectively, in reasonable agreement with the measurements of Knittle et al. (1986).

In summary, the expansivity of (Mg, Fe) SiO_3 perovskite at mantle temperatures is not well-constrained either by experimental observation or theory. The conclusion that the mean expansivity appropriate for the perovskite component of the adiabatically decompressed lower mantle significantly exceeds $3 \times 10^{-5} \text{ K}^{-1}$ is by no means secure. The inference that the mantle must be chemically stratified, with relative enrichment of the lower mantle in silica or iron oxide, is therefore without substantial foundation (Jackson 1983).

Acknowledgements. We are grateful to R.C. Liebermann and A.E. Ringwood for access to the ScAlO_3 specimens, to R.L. Withers for guidance in bond length – bond strength systematics, to R.C. Liebermann for a preview of the unpublished data of Yamanaka et al. (1987), to Z. Guziak for the drafting of the illustrations, and to M. Davern and D. Devir for assistance in the preparation of the manuscript.

References

- Anderson OL (1988) A ferroelectric transition in the lower mantle? EOS (Trans Am Geophys Union) 69:1451
- Anderson OL, Schreiber E, Liebermann RC, Soga N (1968) Some elastic constant data on minerals relevant to geophysics. Rev Geophys 6:491–524
- Bass JD (1984) Elasticity of single-crystal SmAlO_3 , GdAlO_3 and ScAlO_3 perovskites. Phys Earth Planet Inter 36:145–156
- Brown ID, Altermatt D (1985) Bond valence parameters obtained from a systematic analysis of the inorganic crystal structure database. Acta Crystallogr B41:244–247
- Cohen RE (1987) Elasticity and equation of state of MgSiO_3 perovskite. Geophys Res Lett 14:1053–1056
- Hazen RM, Finger LW (1982) Comparative crystal chemistry: temperature, pressure, composition and the variation of crystal structure. Wiley, New York, pp 115–146
- Hazen RM, Prewitt CT (1977) Effects of temperature and pressure on interatomic distances in oxygen-based minerals. Am Mineral 62:309–315
- Hemley RJ, Jackson MD, Gordon RG (1987) Theoretical study of the structure, lattice dynamics and equations of state of perovskite-type MgSiO_3 and CaSiO_3 . Phys Chem Minerals 14:2–12
- Hemley RJ, Cohen RE, Yeganeh-haeri A, Mao HK, Weidner DJ (1989) Raman spectroscopy and lattice dynamics of MgSiO_3 -perovskite at high pressure. In: Navrotsky A, Weidner DJ (eds) Perovskite: a structure of great interest of geophysics and materials science. AGU (Washington), pp 35–44
- Hill RJ (1984) X-ray powder diffraction profile refinement of synthetic hercynite. Am Mineral 69:937–942
- Hill RJ, Howard CJ (1986) A computer program for Rietveld analysis of fixed wavelength x-ray and neutron powder diffraction patterns. Aust. Atomic Energy Comm. (now ANSTO) Report No. M112, 14pp, Lucas Heights Res. Lab., Menai, New South Wales, Australia
- Horiuchi H, Ito E, Weidner DJ (1987) Perovskite-type MgSiO_3 : single-crystal x-ray diffraction study. Am Mineral 72:357–360
- International Tables for X-ray Crystallography (1974) Vol. IV. Kynoch Press, Birmingham (Present distributor D. Reidel, Dordrecht)
- Ito H, Kawada K, Akimoto S (1974) Thermal expansion of stishovite. Phys Earth Planet Inter 8:277–281
- Jackson I (1983) Some geophysical constraints on the chemical composition of the Earth's lower mantle. Earth Planet Sci Lett 62:91–103
- Jeanloz R, Knittle E (1989) Density and composition of the lower mantle. Philos Trans R Soc London A328: 377–389
- Jeanloz R, Thompson AB (1983) Phase transitions and mantle discontinuities. Rev Geophys Space Phys 21:51–74
- Jones LEA (1979) Pressure and temperature dependence of the single crystal elastic moduli of the cubic perovskite KMgF_3 . Phys Chem Minerals 4:23–42
- Knittle E, Jeanloz R, Smith GL (1986) Thermal expansion of silicate perovskite and stratification of the Earth's mantle. Nature 319:214–216
- Liebermann RC, Jones LEA, Ringwood AE (1977) Elasticity of aluminate, titanate, stannate and germanate compounds with the perovskite structure. Phys Earth Planet Inter 14:165–178
- Liu X, Liebermann RC (1988) $A^{2+}B^{4+}O_3$ perovskites at high temperature. EOS (Trans Am Geophys Union) 69:1451
- Liu L, Ringwood AE (1975) Synthesis of a perovskite-type polymorph of CaSiO_3 . Earth Planet Sci Lett 28:209–211
- Liu X, Wang Y, Liebermann RC (1988) Orthorhombic-tetragonal phase transition in CaGeO_3 perovskite at high temperature. Geophys Res Lett 15:1231–1234
- Meagher EP (1975) The crystal structures of pyrope and grossular at elevated temperatures. Am Mineral 60:218–228
- Megaw HD (1971) Crystal structures and thermal expansion. Mater Res Bull 6:1007–1018
- Navrotsky A (1989) Thermochemistry of perovskites. In: Navrotsky A, Weidner DJ (eds) Perovskite: a structure of great interest to geophysics and materials science. AGU (Washington) pp 67–80
- Norrestam P (1969) Refinement of the crystal structure of scandium oxide from single-crystal diffractometer data. Ark Kemi 29:343–349
- Reid AF, Ringwood AE (1975) High-pressure modification of ScAlO_3 and some geophysical implications. J Geophys Res 80:3363–3370
- Rietveld, H.M. (1969) A profile refinement method for nuclear and magnetic structures. J Appl Crystallogr 2:65–71
- Ross NL, Hazen RM (1989) Single-crystal x-ray diffraction study of MgSiO_3 perovskite from 77 to 400 K. Phys Chem Minerals 16:415–420
- Sasaki S, Prewitt CT, Liebermann RC (1983) The crystal structure of CaGeO_3 perovskite and the crystal chemistry of GdFeO_3 -type perovskites. Am Mineral 68:1189–1198
- Sinclair W, Eggleton RA, Ringwood AE (1979) Crystal synthesis and structure refinement of high-pressure ScAlO_3 perovskite. Z Krist 149:307–314
- Skinner BJ (1966) Thermal expansion. In: Clark SP Jr (ed) Handbook of Physical Constants. Geological Society of America Memoir, 97. Geol. Soc. Am., New York, pp 75–96
- Suzuki I, Ohtani E, Kumazawa M (1979) Thermal expansion of γ - Mg_2SiO_4 . J Phys Earth 27:53–61
- Wolf GH, Bukowinski MST (1987) Theoretical study of the structural properties and equations of state of MgSiO_3 and CaSiO_3 perovskites: implications for lower mantle composition. In: Manghnani MH, Syono Y (eds) High pressure research in mineral physics. Terra (Tokyo)/Amer. Geophys. (Washington), pp 313–331
- Wyckoff RWG (1963) Crystal Structures, vol 2. Wiley-Interscience, New York, 588 pp
- Yamanaka T, Prewitt CT, Liebermann RC (1987) High temperature study of ScAlO_3 orthorhombic perovskite. Mineral Soc Jpn (abstract)
- Yeganeh-haeri A, Weidner DJ, Ito E (1989) Elasticity of MgSiO_3 in the perovskite structure. Science 243:787–789